Dilute Bose gases interacting via power-law potentials

Ryan M. Kalas and D. Blume
Department of Physics and Astronomy, Washington State University, Pullman, Washington 99164-2814, USA
(Received 6 November 2007; published 10 March 2008)

Neutral atoms interact through a van der Waals potential which asymptotically falls off as r^{-6}. In ultracold gases, this interaction can be described to a good approximation by the atom-atom scattering length. However, corrections arise that depend on the characteristic length of the van der Waals potential. We parametrize these corrections by analyzing the energies of two- and few-atom systems under external harmonic confinement, obtained by numerically and analytically solving the Schrödinger equation. We generalize our results to particles interacting through a longer-ranged potential which asymptotically falls off as r^{-4}.

DOI: 10.1103/PhysRevA.77.032703 PACS number(s): 34.20.Cf, 03.75.Hh

I. INTRODUCTION

The interaction strengths of sufficiently dilute and cold bosonic atom samples such as Bose-Einstein condensates of alkali-metal atoms can be parametrized to a good approximation by a single parameter, the *s*-wave scattering length [1]. In these systems, the neutral atoms interact through short-ranged van der Waals potentials which fall off as r^{-6} at large interparticle distances r. More recently, progress has been made in cooling and trapping systems characterized by interaction potentials that fall off more slowly than r^{-6} at large r. For example, the interaction between a neutral atom and an ion is dominated by a polarization potential that falls off asymptotically as r^{-4} [2]. Atom-ion systems have recently been proposed as candidates for quantum computing applications [3], and also play a role in recent work which proposes that macroscopic molecules can be formed by immersing an ion in a condensed Bose gas [4–6]. Another example for systems with longer-ranged interactions are dipolar gases [7,8]. In these systems, the non-negligible magnetic or electric dipole moment leads to an angle-dependent r^{-3} potential at large interparticle distances. A natural question to ask is how well the properties of Bose systems with longer-ranged interactions can be described by the *s*-wave scattering length.

This paper considers dilute bosonic systems under external confinement interacting through spherically symmetric power-law potentials. In particular, we treat interactions with r^{-n} tails, where n is 4 or 6. We focus on the regime where the characteristic length β_n of the two-body potential is much smaller than the characteristic length a_{ho} of the trapping potential. In this regime, the shape-dependent interaction potential can be replaced by a regularized zero-range potential whose interaction strength is parametrized by the *s*-wave scattering length. For the potential with r^{-6} tail, e.g., it has been shown previously that the energy levels of the trapped two-body system can be reproduced very accurately if the energy dependence of the scattering length is accounted for [9,10]. This paper extends the two-body analysis to potentials with r^{-4} tail, whose scattering length has—because of the longer-ranged character of the potential—a stronger energy dependence than that of potentials with r^{-6} tail. We find that the corrections to the energy predicted by the zero-energy scattering length go as $(\beta_6/a_{\mathrm{ho}})^3$ and $(\beta_4/a_{\mathrm{ho}})^2$ for the interaction potentials with r^{-6} and r^{-4} tails, respectively.

Using Monte Carlo techniques, we furthermore treat dilute bosonic many-body systems. As in the two-body case, we consider different interaction potentials and analyze the resulting eigenenergies. Not unexpectedly, our results show that the energy-dependent scattering length remains a good quantity also in the many-body system. This suggests, e.g., that the description of dilute Bose gases within a mean-field Gross-Pitaevskii framework can be improved notably by including the energy dependence of the scattering length. First steps in this direction have already been taken [6,11]; our results provide additional benchmark results that may aid in further assessing the accuracy of these and related frameworks.

Section II introduces the Hamiltonian and the model interaction potentials used in our study. Section III discusses the energetics of two particles in a trap interacting through both finite-range and zero-range potentials. In Sec. IV, we consider the energetics of more than two particles in a trap by solving the many-body Schrödinger equation using Monte Carlo techniques. Finally, Sec. V concludes.

II. HAMILTONIAN

The Hamiltonian for a system consisting of N identical mass m bosons in the presence of a spherically symmetric harmonic trapping potential with angular frequency ω is given by

$$H=\sum_{i=1}^{N}\left(-\frac{\hbar^2}{2m}\nabla_i^2+\frac{1}{2}m\omega^2\mathbf{r}_i^2\right)+\sum_{i<j}^{N}v(r_{ij}), \tag{1}$$

where $\mathbf{r}_i$ denotes the position vector of the ith atom. The spherically symmetric two-body interaction potential v depends on the relative distance r_{ij}, $r_{ij}=|\mathbf{r}_i-\mathbf{r}_j|$. We consider attractive power-law potentials with a hardcore radius r_c,

$$v_n(r)=\begin{cases}\infty & \text{for } r<r_c,\\ -C_n/r^n & \text{for } r>r_c,\end{cases} \tag{2}$$

with $n=4,6$ and $C_n>0$. The Hamiltonian defined in Eq. (1) is characterized by three length scales: the hardcore radius r_c, the characteristic length scale β_n [$\beta_n=(mC_n/\hbar^2)^{1/(n-2)}$], and the harmonic oscillator length a_{ho} [$a_{\mathrm{ho}}=\sqrt{\hbar/m\omega}$]. Throughout this paper, we are interested in the regime where r_c and β_n are much smaller than a_{ho}.

In three dimensions, the interaction strength of any potential that falls off faster than r^{-3} at large distances can be characterized by the energy-dependent free-space s-wave scattering length $a(k)$ [17],

$$a(k) = -\frac{\tan \delta(k)}{k}, \tag{3}$$

where $\delta(k)$ denotes the s-wave scattering phase shift and k the wave vector at the scattering energy of $\hbar^2 k^2/m$. The zero-energy scattering length $a(0)$ is defined by taking the $k \to 0$ limit of Eq. (3). For the v_4 and v_6 potentials, the zero energy and energy-dependent scattering lengths can be calculated from analytical solutions derived using series expansion techniques [12,13].

Figures 1(a) and 2(a) show the zero-energy scattering length $a(0)$ as a function of β_n for the v_n potential with $r_c = 0.007 a_{\mathrm{ho}}$ for n equals 4 and 6, respectively. Although the scattering lengths are calculated for the free-space system with no external trapping potential, we choose to express all lengths in units of a_{ho} to ease the comparison with the trapped system in Secs. III and IV. When $\beta_n = 0$, the scattering length coincides with the hardcore radius r_c. As β_n increases, the attractive tails of the v_n potentials increase in strengths, which leads to a decrease of the scattering lengths. This continues until the potential is strong enough to support its first bound state, at which point the scattering length changes its sign from negative to positive. Figures 1(a) and 2(a) indicate that this divergence occurs at different values of β_n, i.e., at $\beta_4 \approx 0.022 a_{\mathrm{ho}}$ and $\beta_6 \approx 0.016 a_{\mathrm{ho}}$, owing to the fact that the v_6 potential is shorter ranged than the v_4 potential. This can be understood heuristically by considering the ratio of the attractive power of the potentials, that is, the ratio $\int v_6(r) d^3\mathbf{r} / \int v_4(r) d^3\mathbf{r}$. Taking the limits of the r integration as r_c and ∞, this ratio equals $\beta_6^4/(3\beta_4^2 r_c^2)$. Looking at equal values of β_4 and β_6 and considering that $\beta_n > r_c$ at the first divergence, this ratio is greater than 1, in agreement with the observation that the v_6 potential supports an s-wave bound state for smaller values of β_n/a_{ho} than the v_4 potential.

Throughout this paper we are interested in describing dilute Bose systems which interact primarily through binary s-wave collisions. In such systems, the short-range details of the interaction potential are not being probed and the regularized zero-range pseudopotential $v_{\mathrm{ps}}(r)$ [14],

$$v_{\mathrm{ps}}(r) = \frac{4\pi\hbar^2}{m} g \delta^{(3)}(\mathbf{r}) \frac{\partial}{\partial r} r \tag{4}$$

reproduces many observables obtained for the true shape-dependent interaction potential—in our case, the v_4 or v_6 potential—accurately if the strength g is chosen properly. In Secs. III and IV we take g to be the zero-energy scattering length $a(0)$ and the energy-dependent scattering length $a(k)$ of the shape-dependent interaction potential v_n.

For two particles in a harmonic trap interacting through v_{ps}, the Schrödinger equation can be solved analytically [15]. The center-of-mass energy equals $(n_{\mathrm{c.m.}} + 3/2)\hbar\omega$ ($n_{\mathrm{c.m.}} = 0, 1, \ldots$), and the s-wave eigenenergies $E_{\mathrm{rel}} = \varepsilon \hbar\omega$ of the Schrödinger equation in the relative coordinate are determined by [15]

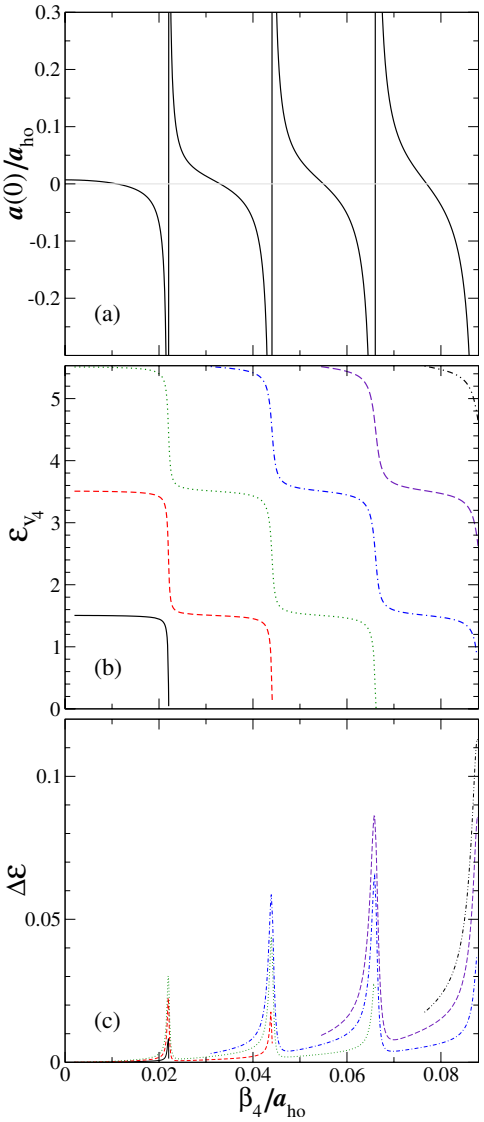

FIG. 1. (Color online) s-wave properties of two particles interacting through the potential v_4 with $r_c = 0.007 a_{\mathrm{ho}}$ as a function of β_4/a_{ho} (note that the x axis is the same for all three panels): (a) Free-space zero-energy scattering length $a(0)$. (b) Relative energy ε_{v_4} for two trapped atoms. (c) Energy difference $\Delta\varepsilon$, $\Delta\varepsilon = \varepsilon_{v_4} - \varepsilon_{a(0)}$, for two trapped atoms. In (b) and (c), the line styles are keyed to each other for ease of comparison.

$$\frac{g}{a_{\mathrm{ho}}} = \frac{\Gamma\left(-\frac{\varepsilon}{2} + \frac{1}{4}\right)}{\sqrt{2}\Gamma\left(-\frac{\varepsilon}{2} + \frac{3}{4}\right)}. \tag{5}$$

The transcendental Eq. (5) can be solved straightforwardly for any given g using standard root-finding procedures. For $N > 2$, analytical solutions to the Schrödinger equation for trapped atoms interacting through v_{ps} are in general not known, and we instead resort to numerical techniques (see Sec. IV).

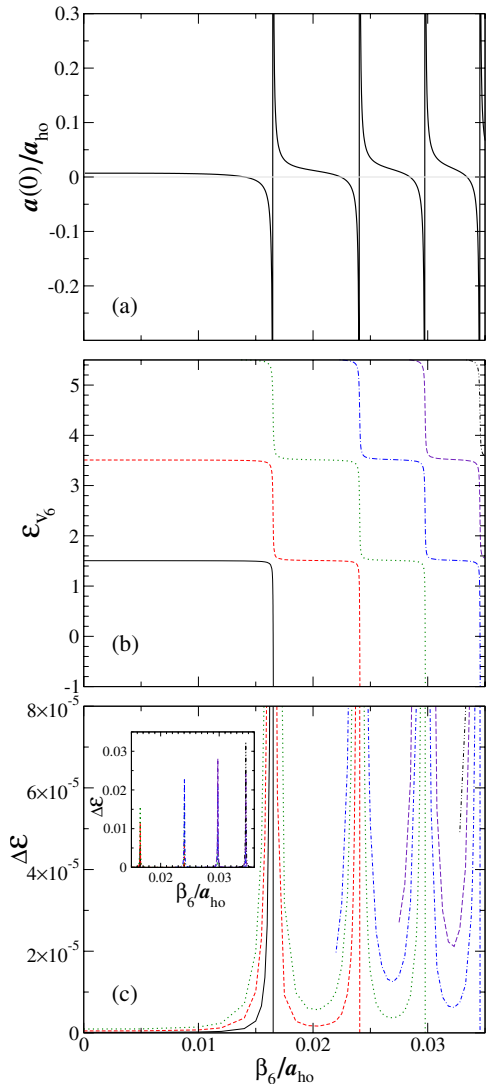

FIG. 2. (Color online) s-wave properties of two particles interacting through the potential v_6 with $r_c=0.007a_{\rm ho}$ as a function of $\beta_6/a_{\rm ho}$ (note that the x axis is the same for all three panels): (a) Free-space zero-energy scattering length $a(0)$. (b) Relative energy ε_{v_6} for two trapped atoms. (c) Energy difference $\Delta\varepsilon$, $\Delta\varepsilon=\varepsilon_{v_6}-\varepsilon_{a(0)}$, for two trapped atoms. The inset of (c) plots $\Delta\varepsilon$ on an enlarged scale to show the maximum of $\Delta\varepsilon$. In (b) and (c), the line styles are keyed to each other for ease of comparison.

III. TWO PARTICLES IN A TRAP

We first consider the Hamiltonian given in Eq. (1) with $v=v_n$ for $N=2$. After separating off the center of mass motion, we are left with a Schrödinger equation in the relative coordinate. We solve the corresponding one-dimensional differential equation numerically using B splines. Figures 1(b) and 2(b) show the resulting relative s-wave eigenenergies, denoted by ε_{v_4} and ε_{v_6}, respectively, as a function of β_n. As in Figs. 1(a) and 2(a), the hardcore radius is fixed at $r_c=0.007a_{\rm ho}$. For those β_n values for which $a(0)$ is small [see Figs. 1(a) and 2(a)], the eigenenergies ε_{v_n} coincide approximately with the eigenenergies $(2n_{\rm rel}+3/2)$ of the noninteracting system, where $n_{\rm rel}=0,1,\ldots$. However, each time $a(0)$ diverges, a new molecular state appears and the energy of the gaslike state decreases by approximately $2\hbar\omega$.

Next, we consider two trapped particles interacting through $v_{\rm ps}$. We find that the zero-range pseudopotential with energy-dependent scattering length reproduces the eigenenergies ε_{v_n} for the shape-dependent potential v_n with high accuracy for all interaction strengths considered in Figs. 1 and 2. To obtain the eigenenergies for $v_{\rm ps}$ with $g=a(k)$, which we denote by $\varepsilon_{a(\varepsilon)}$, we calculate $a(k)$ for different β_n and solve Eq. (5) self-consistently [9,10], i.e., we require that $\varepsilon\hbar\omega$ on the right-hand side of Eq. (5) agrees with the energy $\hbar^2k^2/m$ at which the two particles collide. Since ε_{v_n} and $\varepsilon_{a(\varepsilon)}$ coincide to many digits, Eq. (5) can be used to describe the physics of two trapped particles provided $\beta_n \ll a_{\rm ho}$ and provided the energy dependence of the scattering length is known. For short-range potentials, this was already shown in Refs. [9,10]. For some systems under experimental study, only $a(0)$ is known [$a(k)$ is unknown]. It is thus useful to quantify the deviations $\Delta\varepsilon$ between the eigenenergies ε_{v_n} and the eigenenergies $\varepsilon_{a(0)}$ obtained from Eq. (5) with $g=a(0)$.

Figures 1(c) and 2(c) show the energy difference $\Delta\varepsilon$, $\Delta\varepsilon=\varepsilon_{v_n}-\varepsilon_{a(0)}$, for the three energetically lowest-lying gaslike states. The line styles in Figs. 1(c) and 2(c) correspond to those used in Figs. 1(b) and 2(b). The energy difference $\Delta\varepsilon$ is larger for the energetically higher-lying gaslike states since the energy dependence of $a(k)$ for a given β_n increases with increasing ε. The maximum of $\Delta\varepsilon$ increases with increasing $\beta_n/a_{\rm ho}$ [see Fig. 1(c) and the inset of Fig. 2(c)] and is of the same order of magnitude for the v_4 and v_6 potentials for comparable values of $\beta_n/a_{\rm ho}$. Furthermore, for those β_n values for which the scattering length $a(0)$ is comparatively small, the energy difference $\Delta\varepsilon$ also increases with increasing $\beta_n/a_{\rm ho}$. The magnitude of these "background" energy differences is much larger for the v_4 potential than for the v_6 potential [note the difference in the y scales of Figs. 1(c) and 2(c)]. For example, for $\beta_n\approx 0.03a_{\rm ho}$, the background energy is about $10^{-3}\hbar\omega$ and $10^{-5}\hbar\omega$ for the lowest-lying gaslike states of the v_4 and v_6 potentials, respectively. We now show that the background energy difference $\Delta\varepsilon$ is proportional to $(\beta_4/a_{\rm ho})^2$ and $(\beta_6/a_{\rm ho})^3$ for the v_4 and v_6 potentials, respectively, thus explaining the much smaller energy difference for the v_6 potential than for the v_4 potential.

To arrive at these estimates, we use that $\varepsilon_{a(\varepsilon)}$ agrees to many digits with ε_{v_n}, which implies $\Delta\varepsilon=\varepsilon_{a(\varepsilon)}-\varepsilon_{a(0)}$. Since $\varepsilon_{a(\varepsilon)}$ is determined from Eq. (5) with $g=a(\varepsilon)$, we can obtain a simple expression for $\varepsilon_{a(\varepsilon)}$ by expanding the left-hand side of Eq. (5) about $a(0)$ and the right-hand side about $\varepsilon_{a(0)}$. The expansions of $a(k)$ for the v_4 and the v_6 potentials are given by [16]

$$a(k) = a(0) + \frac{\pi}{3}\beta_4^2 k + \cdots \tag{6}$$

and [17]

$$a(k) = a(0)\left(1 + \frac{1}{2}r_e a(0)k^2 + \cdots\right), \tag{7}$$

respectively. In Eq. (7), r_e denotes the effective range of the v_6 potential [11,18],

$$\frac{r_e}{\beta_6} = \frac{2}{3x_e}\frac{1}{[a(0)/\beta_6]^2}\left[1+\left(1-x_e\frac{a(0)}{\beta_6}\right)^2\right], \tag{8}$$

where the constant $x_e=[\Gamma(1/4)]^2/(2\pi)\approx 2.09$. Denoting the right-hand side of Eq. (5) by $f(\varepsilon_{a(0)})$ for $g=a(0)$, we find

$$\Delta\varepsilon \approx \frac{\frac{\pi}{3}\left(\frac{\beta_4}{a_{ho}}\right)^2\sqrt{\varepsilon_{a(0)}}}{f'(\varepsilon_{a(0)})-\frac{\pi}{3}\left(\frac{\beta_4}{a_{ho}}\right)^2\sqrt{\varepsilon_{a(0)}}} \tag{9}$$

for the v_4 potential and

$$\Delta\varepsilon \approx \frac{\frac{1}{2}\frac{r_e}{a_{ho}}\left(\frac{a(0)}{a_{ho}}\right)^2\varepsilon_{a(0)}}{f'(\varepsilon_{a(0)})-\frac{1}{2}\frac{r_e}{a_{ho}}\left(\frac{a(0)}{a_{ho}}\right)^2\varepsilon_{a(0)}} \tag{10}$$

for the v_6 potential. The different powers of $\varepsilon_{a(0)}$ in Eqs. (9) and (10) follow directly from the linear and quadratic k dependence of the correction terms in Eqs. (6) and (7), respectively.

If $a(0)\ll\beta_6$, the square bracket in the expression for the effective range r_e is approximately equal to 2 and Eq. (10) reduces to

$$\Delta\varepsilon \approx \frac{\frac{2}{3x_e}\left(\frac{\beta_6}{a_{ho}}\right)^3\varepsilon_{a(0)}}{f'(\varepsilon_{a(0)})-\frac{2}{3x_e}\left(\frac{\beta_6}{a_{ho}}\right)^3\varepsilon_{a(0)}}. \tag{11}$$

Furthermore, for small $a(0)$, $\varepsilon_{a(0)}$ is approximately given by $(3/2+2n_{\mathrm{rel}})$ and $f'(\varepsilon_{a(0)})$ is of order 1 (taking values of approximately 1.25, 0.84, and 0.67 for $n_{\mathrm{rel}}=0$, 1, and 2). The second term in the denominator of Eqs. (9) and (11) can thus be dropped provided β_n is much smaller than a_{ho}. This yields

$$\Delta\varepsilon \approx \frac{\pi\sqrt{2n_{\mathrm{rel}}+3/2}}{3f'(2n_{\mathrm{rel}}+3/2)}\left(\frac{\beta_4}{a_{\mathrm{ho}}}\right)^2 \tag{12}$$

for the v_4 potential and

$$\Delta\varepsilon \approx \frac{2(2n_{\mathrm{rel}}+3/2)}{3x_e f'(2n_{\mathrm{rel}}+3/2)}\left(\frac{\beta_6}{a_{\mathrm{ho}}}\right)^3 \tag{13}$$

for the v_6 potential. Equations (12) and (13) can also be derived by applying first order perturbation theory to the trapped two-body system interacting through a zero-range potential (see Sec. IV).

Solid and dotted lines in Fig. 3 show the energy differences $\Delta\varepsilon$ predicted by Eqs. (13) and (12) for $n_{\mathrm{rel}}=0$, 1, and 2 (from bottom to top) as a function of β_n/a_{ho} for the v_6 and v_4 potentials, respectively. For comparison, filled and open symbols in Fig. 3 show the corresponding numerically determined energy differences $\Delta\varepsilon$ for the three energetically lowest-lying gaslike states. To calculate these energy differences, we fix r_c and β_n so that $a(0)=0$, and vary the harmonic oscillator length. We find that, as long as r_c and $\beta_n \ll a_{\mathrm{ho}}$, the results shown in Fig. 3 are independent of the number of bound states supported by the shape-dependent power-law potential v_n. Figure 3 illustrates that the estimates given in Eqs. (12) and (13) are quite accurate for small $a(0)$. Thus, our derivation shows that the different powers of the characteristic length scale β_n, which explain the larger background values of $\Delta\varepsilon$ for the v_4 potential compared to the v_6 potential, can be traced back to the different energy dependence of $a(k)$ for the v_4 and v_6 potentials.

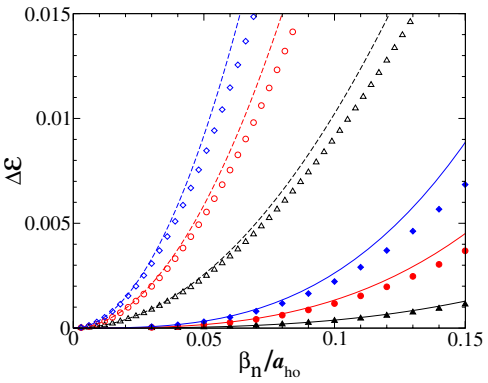

FIG. 3. (Color online) Energy difference $\Delta\varepsilon$, $\Delta\varepsilon=\varepsilon_{v_n}-\varepsilon_{a(0)}$, for the three energetically lowest-lying gaslike states of two trapped atoms for $a(0)=0$ as a function of β_n/a_{ho}. The filled (open) triangles, circles, and diamonds show the numerically determined energy differences for the levels near 1.5, 3.5, and $5.5\hbar\omega$, respectively, for the v_6 (v_4) potential. The solid and dashed lines show the corresponding analytically determined estimates for $\Delta\varepsilon$, Eqs. (13) and (12).

IV. N PARTICLES IN A TRAP

To solve the time-independent Schrödinger equation for more than $N=2$ trapped particles, we resort to the variational Monte Carlo (VMC) and diffusion Monte Carlo (DMC) techniques [19]. In the VMC method, the variational many-body wave function ψ_V is written in terms of a set of variational parameters $\mathbf{p}$, which are optimized so as to minimize the variational energy E_V, $E_V=\langle\psi_V|H|\psi_V\rangle/\langle\psi_V|\psi_V\rangle$. The energy expectation value E_V is calculated for a given $\mathbf{p}$ using Metropolis sampling. Motivated by the structure of the Hamiltonian H, Eq. (1), we write ψ_V as a product of one-body terms φ and two-body Jastrow terms F [20–22],

$$\psi_V(\mathbf{r}_1,\ldots,\mathbf{r}_N)=\prod_{i=1}^{N}\varphi(r_i)\prod_{i<j}^{N}F(r_{ij}), \tag{14}$$

where $\varphi(r)=\exp(-p_1 r^{p_2})$. The functional form of the two-body Jastrow factor F is motivated by the functional form of the interaction potential v and by the fact that we are interested in describing the energetically lowest-lying gaslike state of the many-body Hamiltonian. We use

$$F(r)=\begin{cases}(1-b/r)(1+p_3/r^{p_4}) & \text{for } r>b,\\ 0 & \text{for } r\le b,\end{cases} \tag{15}$$

for $v=v_n$, and

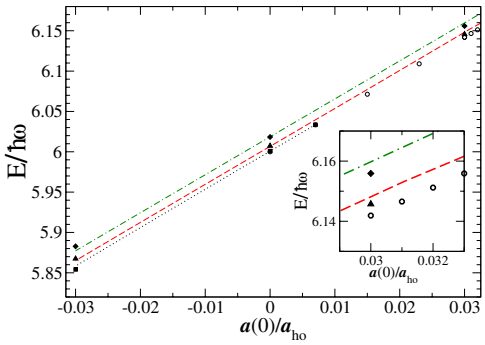

FIG. 4. (Color online) Solid squares, triangles, and diamonds show the total energy $E_{v_4}(N)$ calculated by the DMC method for four trapped particles interacting through the v_4 potential with $r_c=0.007a_{\rm ho}$ as a function of $a(0)/a_{\rm ho}$. The dotted, dashed, and dash-dotted lines show the perturbative energies, Eq. (17), for two-body potentials that support 0, 1, and 2 bound states. No solid squares are shown for $a(0)>r_c$ because the largest scattering length for the v_4 potential that supports no bound state equals r_c; in this case, $C_4=0$. Open circles show the total energy $E_{a(0)}(N)$ calculated by the DMC method for four particles interacting through the zero-range pseudopotential $v_{\rm ps}$ with $g=a(0)$. For $a(0)=0$ and $0.007a_{\rm ho}$, the open circles are indistinguishable from the solid squares on the scale shown. For all cases, the error bars of the energies are smaller than the symbol size. The inset shows an enlargement of the region around $a(0)=0.03a_{\rm ho}$.

$$F(r)=\begin{cases}0 & \text{for } r\le c,\\ \sin(kr+d) & \text{for } c<r\le p_5,\\ e_1+e_2\exp(-p_6 r) & \text{for } r>p_5,\end{cases} \tag{16}$$

for $v=v_{\rm ps}$. The parameters b, c, d, and k are chosen so that ψ_V obeys the boundary conditions implied by the many-body Hamiltonian H and so that ψ_V has the desired symmetry (see below), while the parameters e_1 and e_2 are determined by requiring that F and its derivative are continuous at $r=p_5$. For each interaction potential v, we optimize the variational parameters $\mathbf{p}$, i.e., p_1 through p_4 for $v=v_n$, and p_1, p_2, p_5, and p_6 for $v=v_{ps}$.

To go beyond the variational calculations, we apply two different variants of the DMC algorithm both of which use the optimized wave function ψ_V as a guiding function [19]. When the many-body Hamiltonian does not support any states with negative energy, the lowest-lying gaslike state coincides with the true ground state of the system. In this case, ψ_V is nodeless and the DMC algorithm with importance sampling results in the exact many-body energy. When the many-body Hamiltonian supports negative energy states, i.e., molecularlike bound states, the energetically lowest-lying gaslike state possesses nodes, which are imposed in the DMC method with importance sampling through the variational wave function ψ_V. This DMC variant, referred to as the fixed-node DMC method [19,23], determines the lowest energy of a state that has the same symmetry as ψ_V. Importantly, the FN-DMC energy provides an upper bound to the exact eigenenergy of the excited gaslike state of the many-body system [23].

The solid squares, triangles, and diamonds in Fig. 4 show the total energy $E_{v_4}(N)$ calculated by the DMC method for $N=4$ trapped particles interacting through the v_4 potential with $r_c=0.007a_{\rm ho}$ as a function of the zero-energy scattering length $a(0)$ for a varying number of two-body s-wave bound states. The solid squares show energies for two-body potentials that support no s-wave bound state. For the two-body potentials considered, the corresponding four-body system supports no state with negative energy, and the hardcore boundary condition implied by v_4 is met by setting the parameter b in Eq. (15) equal to r_c. The energies for those v_4 potentials that support one and two s-wave bound states are shown by solid triangles and diamonds, respectively. In these cases, the four-particle system supports negative energy states, and the parameter b is chosen to coincide with the r value at which the free-space zero-energy two-body scattering solution has its first and second node, respectively. This construction of the many-body nodal surface assumes that at most two particles scatter at any given time, and that the nodal line of the two-body scattering solution is not modified by the presence of the other atoms [24,25]. This "binary approximation" is expected to be quite accurate in the low-density regime considered throughout this paper. Figure 4 shows that, for a given zero-energy scattering length $a(0)$, the energy E_{v_4} of the lowest-lying gaslike state increases as the number of two-body s-wave bound states or, equivalently, $\beta_4/a_{\rm ho}$ increases, similar to the behavior found in Sec. II for the two particle case [see Fig. 1(c)].

For comparison, we consider the energy of N particles interacting through an energy-dependent zero-range pseudopotential, within first order perturbation theory

$$\frac{E(N)}{\hbar\omega}=\frac{3}{2}N+\frac{N(N-1)}{2}\sqrt{\frac{2}{\pi}}\frac{a(k)}{a_{\rm ho}}. \tag{17}$$

For weakly interacting systems, i.e., for small scattering lengths, $a(k)$ can be approximated by Eq. (6) with k corresponding to the trap energy scale of $3/2\hbar\omega$. The perturbative results for $N=4$ particles are shown in Fig. 4 by dotted, dashed, and dash-dotted lines for the cases when the two-body potential supports zero, one, and two bound states. The agreement between the perturbative and DMC energies is reasonably good over the range of scattering lengths considered. In particular, the perturbative expression with the energy-dependent scattering length predicts the up-shift of the energies with increasing number of two-body bound states for a fixed $a(0)$ correctly but does not fully capture the change of slope of the energy with increasing $|a(0)|$.

Next we consider the DMC and FN-DMC results for N trapped atoms interacting through the pseudopotential $v_{\rm ps}$ with $g=a(0)$. The potential $v_{\rm ps}$ possesses one two-body bound state for $g>0$ and no two-body bound state for $g<0$. For positive scattering lengths, we thus use the FN-DMC method. The nodes of F, Eq. (16), are determined by the free-space two-body scattering solution for $v_{\rm ps}$, i.e., we use $c=a(0)$ and $d=\delta(0)$ (for numerical reasons, we take a finite k, $k\ll a_{\rm ho}^{-1}$, and check that the results are independent of the actual k value used). In addition to positive $a(0)$, we consider negative $a(0)$. Since the pseudopotential possesses no two-body bound state in this case, we use the DMC rather

than the FN-DMC method. Using ψ_V with $c=0$, and d and k chosen so that the boundary condition implied by the zero-range pseudopotential is satisfied whenever one of the interparticle distances r_{ij} is zero, numerical instabilities associated with large negative DMC energies arise. These instabilities are most likely associated with the Thomas collapse [26,27], which is known to occur for systems with three or more particles interacting through $v_{\rm ps}$ with $g<0$.

The open circles in Fig. 4 show the total DMC energy $E_{a(0)}(4)$ as a function of the zero-energy scattering length $a(0)$ for $a(0)\geq 0$. We find that $E_{a(0)}(4)$ is smaller than or equal to $E_{v_4}(4)$ for all $a(0)$. To quantify to which extent the Hamiltonian with the shape-independent potential reproduces the properties of the Hamiltonian with the shape-dependent potential, we consider the energy difference $\Delta E(N)$, $\Delta E(N)=E_{v_4}(N)-E_{a(0)}(N)$. For $N=4$ and 10, we find that ΔE scales—as might be expected for a weakly interacting Bose gas—with the number of pairs, i.e., $\Delta E(N)/\hbar\omega \approx N_{\rm pair}\Delta\varepsilon_{v_4}$, where $\Delta\varepsilon_{v_4}$ denotes the energy difference introduced in Sec. III and $N_{\rm pair}$ the number of pairs, $N_{\rm pair}=N(N-1)/2$. For $N=4$ and $a(0)=0.03a_{\rm ho}$, e.g., we find $E_{v_4}=6.1457(2)\hbar\omega$ (triangles in the inset of Fig. 4) for the v_4 potential that supports one two-body s-wave bound state and $E_{a(0)}=6.14189(3)\hbar\omega$ (open circles in the inset of Fig. 4) for the zero-range potential with $g=a(0)$, and thus $\Delta E=0.0038(2)\hbar\omega$. For comparison, the corresponding quantity $N_{\rm pair}\Delta\varepsilon$ equals $0.0040\hbar\omega$. In addition to the v_4 potential, we consider the v_6 potential. In this case, the energy difference ΔE for comparatively small $a(0)$ is of the same order or larger than the statistical uncertainties of our DMC energies and, although expected to be valid, we cannot explicitly confirm the scaling of ΔE with $N_{\rm pair}$ for the v_6 potential.

To further understand the implications of the energy-dependent scattering length $a(E)$ for $N>2$, we determine the $a(E)$ that, if used to parametrize the interaction strength of the zero-range potential in the many-body Hamiltonian, reproduces the energy E_{v_4}. For example, to reproduce the four-particle energy $E_{v_4}=6.1457(2)\hbar\omega$ for the v_4 potential with $a(0)=0.03a_{\rm ho}$ that supports one bound state, the strength of the pseudopotential has to be $a(E)=0.03082(4)a_{\rm ho}$. For the v_4 potential, this $a(E)$ corresponds to a two-body scattering energy of $1.53(16)\hbar\omega$. Thus, the relevant scattering energy for two-body collisions occurring in the weakly interacting many-body system is, not unexpectedly, approximately given by the trap energy scale of $3/2\hbar\omega$.

V. CONCLUSION

This paper studies trapped bosons interacting through attractive power-law potentials with r^{-4} and r^{-6} tails. For two particles, the energy-dependent pseudopotential accurately reproduces the energies for both shape-dependent potentials. Further, we find that the deviations between the energies obtained for the energy-independent pseudopotential and the shape-dependent potential scale for small $a(0)$ as $(\beta_6/a_{\rm ho})^3$ and $(\beta_4/a_{\rm ho})^2$ for the potentials with r^{-6} and r^{-4} tails, respectively. Finally, we use Monte Carlo methods to extend the treatment to more than two trapped particles. Again, we find that the energy for the shape-dependent power-law potential can be reproduced accurately by the energy-dependent pseudopotential if the energy scale entering the pseudopotential is chosen properly. In general, this leads to a self-consistent many-body framework that considers only binary interactions but includes many-body correlations.

Even if the r^{-4} results are not directly applicable to present-day experiments (combined atom-ion systems have not yet been trapped), our comparative study of the energetics for r^{-4} and r^{-6} potentials provides insights into weakly interacting systems in general and van der Waals r^{-6} interactions in particular. Our calculations suggest that three-body terms [28] are very small in the dilute limit considered throughout this work. It seems feasible that the description of systems with longer-ranged interactions at the mean-field level can be improved by including the energy dependence of the scattering length, similar to the frameworks outlined in Refs. [6,11].

ACKNOWLEDGMENT

We gratefully acknowledge support by the NSF through Grant No. PHY-0555316.

[1] C. J. Pethick and H. Smith, *Bose-Einstein Condensation in Dilute Gases* (Cambridge University Press, Cambridge, 2001).
[2] B. H. Bransden and C. J. Joachain, *Physics of Atoms and Molecules*, 2nd ed. (Prentice Hall, Upper Saddle River, NJ, 2003).
[3] Z. Idziaszek, T. Calarco, and P. Zoller, Phys. Rev. A **76**, 033409 (2007).
[4] R. Coté, V. Kharchenko, and M. D. Lukin, Phys. Rev. Lett. **89**, 093001 (2002).
[5] P. Massignan, C. J. Pethick, and H. Smith, Phys. Rev. A **71**, 023606 (2005).
[6] A. Collin, P. Massignan, and C. J. Pethick, Phys. Rev. A **75**, 013615 (2007).
[7] L. Santos, G. V. Shlyapnikov, P. Zoller, and M. Lewenstein, Phys. Rev. Lett. **85**, 1791 (2000).
[8] A. Griesmaier, J. Werner, S. Hensler, J. Stuhler, and T. Pfau, Phys. Rev. Lett. **94**, 160401 (2005).
[9] D. Blume and C. H. Greene, Phys. Rev. A **65**, 043613 (2002).
[10] E. L. Bolda, E. Tiesinga, and P. S. Julienne, Phys. Rev. A **66**, 013403 (2002).
[11] H. Fu, Y. Wang, and B. Gao, Phys. Rev. A **67**, 053612 (2003).
[12] N. A. W. Holzwarth, J. Math. Phys. **14**, 191 (1973), and references therein.
[13] B. Gao, Phys. Rev. A **58**, 1728 (1998).
[14] K. Huang and C. N. Yang, Phys. Rev. **105**, 767 (1957).
[15] T. Busch, B.-G. Englert, K. Rzażewski, and M. Wilkens, Found. Phys. **28**, 549 (1998).

[16] T. F. O'Malley, L. Spruch, and L. Rosenberg, J. Math. Phys. **2**, 491 (1961). The next terms in the expansion of Eq. (6) are of order k^2 and $k^2 \ln(k\beta_4)$.
[17] R. G. Newton, *Scattering Theory* (Dover, New York, 2002).
[18] B. Gao, Phys. Rev. A **58**, 4222 (1998).
[19] B. L. Hammond, W. A. Lester, Jr., and P. J. Reynolds, *Monte Carlo Methods in Ab Initio Quantum Chemistry* (World Scientific, Singapore, 1994).
[20] R. Jastrow, Phys. Rev. **98**, 1479 (1955).
[21] J. L. DuBois and H. R. Glyde, Phys. Rev. A **63**, 023602 (2001).
[22] D. Blume and C. H. Greene, Phys. Rev. A **63**, 063601 (2001).
[23] P. J. Reynolds, D. M. Ceperley, B. J. Alder, and W. A. Lester, Jr., J. Chem. Phys. **77**, 5593 (1982).
[24] G. E. Astrakharchik, D. Blume, S. Giorgini, and B. E. Granger, J. Phys. B **37**, S205 (2004).
[25] I. Khan and B. Gao, Phys. Rev. A **73**, 063619 (2006).
[26] L. H. Thomas, Phys. Rev. **47**, 903 (1935).
[27] D. V. Fedorov and A. S. Jensen, Phys. Rev. A **63**, 063608 (2001).
[28] T. T. Wu, Phys. Rev. **115**, 1390 (1959).